

New synthesized bismuth-based pyrochlore compounds $\text{Bi}_{1.5-x}\text{M}_x\text{Sb}_{1.5-x}\text{M}'_x\text{ZnO}_7$ (M= Fe; M'=Fe, Cr) (x=0.0; 0.10; 0.15): A structural study.

Karima Ezziane ¹, Mayouf Sellami ¹, Mostefa Kameche ^{2*}, Nourredine Bettahar ¹, Fadia Merabet ¹

¹ Laboratory of Inorganic Materials Chemistry and Application, Department of Materials Engineering, Faculty of Chemistry, University of Sciences and Technology of Oran, P.O. Box 1505, M'Nouar, 31000, Oran, Algeria.

² Laboratory of Physical-Chemistry of Materials, Catalysis and Environment, Faculty of Chemistry, University of Sciences and Technology of Oran, P.O. Box 1505, M'Nouar, 31000, Oran, Algeria.

Abstract

New limited pyrochlore solid solutions of formula $\text{Bi}_{1.5-x}\text{M}_x\text{Sb}_{1.5-x}\text{M}'_x\text{ZnO}_7$ (M= Fe; M'=Fe, Cr) (x=0; 0.10; 0.15) are prepared from simple oxides at 1080°C by using the ceramic method. All the crystal phases are indexed in the cubic system (space group; No.227). Rietveld refinement method of the $\text{Bi}_{1.5}\text{Sb}_{1.5}\text{ZnO}_7$ (x=0) compounds using powder XRD analysis confirms an overall $\text{A}_2\text{B}_2\text{O}_7$ cubic pyrochlore structure according to $(\text{Bi}_{1.5}^{3+}\text{Zn}_{0.5}^{2+})(\text{Sb}_{1.5}^{5+}\text{Zn}_{0.5}^{2+})\text{O}_7$ formula with 10.44425(3) Å and Fd $\bar{3}$ m space group. The substitution of Bi(III) and Sb(V) by Fe(III) and Cr(III) in the $\text{Bi}_{1.5}\text{Sb}_{1.5}\text{ZnO}_7$ phase shows the appearance of solid solutions limited to x=0.15. The variation of the cell's parameter is recorded to the element's ionic radii. The paramagnetic character is observed in all substituted compounds. The measurements of the electrical conductivity as a function of the temperature, make evidence of the semi-conductive property. Whilst, the magnetic susceptibility satisfies the modified Curie Weiss (CW) and shows the magnetic behavior due to the magnetic moments of the iron and chromium ions being involved in the synthesis of the compounds. Besides, the UV-Visible reflectance displays light absorption in the visible domain.

Keywords: Pyrochlore, Oxides, Solid Solution, Magnetic susceptibility, Electric Conductivity.


INTRODUCTION

Pyrochlore-type minerals are a family of compounds with a wide variety of chemical compositions of considerable interest, remarkable advantages, and variable physical properties. Their general formula is written in the form $\text{A}_2\text{B}_2\text{O}_6\text{O}'$ or $\text{A}_2\text{B}_2\text{O}_6\text{X}$ (X being an anion), with "A" stands for relatively large mono-, bi- or trivalent cation such as Bi^{+3} (La, Ca, K, Ba, Y, Ce, Sr, ...etc.), in coordination 8 and a radius often greater than 1 Å, "B" for smaller cation such as Zn^{+2} (Sb, Nb, Ta, Ti, Sn, ...etc.), in coordination 6. The position of the seventh anion (X) in the crystalline structure can be occupied by the anion O^{2-} , OH^- , or F^- [1]. They are face-centered cubic symmetry materials with 8 molecules per cell. The structure can be considered the nesting of the two relatively interdependent networks [2-4], where the oxygen atoms are in two different networks: $\text{A}_2\text{O}'$ tetrahedral and B_2O_6 octahedral. There are two types of sublattices: $\text{A}_2\text{O}'$ where the cation "A" is in coordination 8 (with 2 O' atoms and 6 O atoms) inside a rhombohedron and B_2O_6 where the cation "B" is in octahedral coordination and shares vertices to form larger cavities [5]. Previous studies have shown that the $\text{Bi}_{1.5}\text{Sb}_{1.5}\text{CuO}_7$ compound has a pyrochlore-like structure where the copper is distributed between the sites A and B according to the formula $(\text{Bi}_{1.5}\text{Cu}_{0.5})(\text{Sb}_{1.5}\text{Cu}_{0.5})\text{O}_7$ [3]. Whilst other compounds display similar organization typical of a pyrochlore with zinc i.e. $(\text{Bi}_{1.5}\text{Zn}_{0.5})(\text{Sb}_{1.5}\text{Zn}_{0.5})\text{O}_7$

[6, 7] or $(\text{Bi}_{1.5}\text{Zn}_{0.5})(\text{Nb}_{1.5}\text{Zn}_{0.5})\text{O}_7$ [8, 9] or compounds with manganese $\text{Bi}_{1.5}\text{Sb}_{1.5-x}\text{Nb}_x\text{MnO}_7$ [10] and cobalt $(\text{Bi}_{1.56}\text{Co}_{0.44})(\text{Sb}_{1.48}\text{Co}_{0.52})\text{O}_7$ [11] or finally $(\text{Bi}_{1.56}\text{Co}_{0.44})(\text{Sb}_{1.48-x}\text{Nb}_x\text{Co}_{0.52})\text{O}_7$ [12].

The properties of these materials often change with temperature [1, 6, 14-16]; they can be used therefore in different fields, such as ferroelectricity (as ionic conductors), or mixed conductors (ionic and electronic) in particular as metallic conductors, semi-conductors or even superconductors [17-21]. They exhibit oxygen conductivity that allows them to be utilized in solid electrolyte fuel cells [22, 23]. Besides, they have dielectric, piezoelectric, ferromagnetic, and anti-ferromagnetic properties [24-32]. Their sensitive photocatalytic behavior towards visible light, [33, 34], high magnetoresistance [35, 36], and host matrix of nuclear waste [37, 38] have been proven. With such materials, it is possible to produce novel solid pyrochlore solutions by substituting cations at sites A and/or B under certain experimental operating conditions [6]. Moreover, it may be noticed that non-oxidized pyrochlore structures based on chlorides and fluorides have been demonstrated [39, 40]. Recently, a new solid solution of pyrochlore-type cobalt oxide was synthesized with the chemical formula $\text{Bi}_{1.56-x}\text{Ca}_x\text{Sb}_{1.48}\text{Co}_{0.96}\text{O}_{7-\delta}$ and proved very interesting physical properties [41]. Based on this study, a further investigation has been carried on by using the new synthesized bismuth-based pyrochlore compounds.

In the present study, the substitution of bismuth/antimony by iron/chromium on the structural and magnetic/electrical properties in solid solutions that derive from the $\text{Bi}_{1.5}\text{Sb}_{1.5}\text{ZnO}_7$ phase [7] was investigated. The phases

* mostefa.kameche@univ-usto.dz; kameche@hotmail.com
 <https://orcid.org/0000-0002-0613-0717>

studied were in the form $\text{Bi}_{1.5-x}\text{M}_x\text{Sb}_{1.5-x}\text{M}'_x\text{ZnO}_7$ ($\text{M} = \text{Fe}$; $\text{M}' = \text{Fe, Cr}$) ($x=0.10$; 0.15) and were synthesized using the ceramic method at high temperatures; x being the rate of substitution. All the compounds obtained were characterized by XRD, SEM, FTIR, and UV-Vis reflectance spectroscopy. In addition, the magnetic and electrical properties were also carried out to determine their physical properties.

EXPERIMENTAL

The materials were prepared by reaction in the solid state and subsequently limited solid solutions were obtained by taking the pyrochlore compound base of formula $\text{Bi}_{1.5}\text{Sb}_{1.5}\text{ZnO}_7$ as recommended elsewhere [7]. A series of microcrystalline samples of mass 2 g each were prepared, in solid and under air state conditions separately, from the stoichiometric mixtures of the precursor oxides Bi_2O_3 (99.9%), ZnO (99.9%), Sb_2O_3 (99.9%), Fe_2O_3 (99.9%), and Cr_2O_3 (99.9%) (Aldrich Chemical Company Ltd). Before heating, the mixtures were ground in an agate mortar, pestled for 1 hour, and then placed in sintered alumina crucibles. A first heating was carried out at 700°C for 24 hours (well below the melting point of Bi_2O_3 , 825°C), followed by a second heating at 900°C for 72 hours. The third heating was carried out at 1000°C for 24 hours and finally, the samples were then made in a mortar in the form of pellets approximately 10 mm in diameter and 2 mm in thickness by applying a pressure of 400 kgf/cm^2 , to undergo a final sintering treatment at 1080°C for 48 hours. At the end, the samples were cooled to room temperature and taken out from the oven. Between two heat treatments, homogenization grinding was necessary and as a general rule, all these intermediate procedures of heating have been carried out to achieve the complete reaction between the starting oxides.

After having been synthesized and elaborated, the samples were then characterized by X-ray powder Diffraction (XRD) using a diffractometer (Siemens D5000) operating in Bragg-Brentano type focusing geometry (θ/θ) with the wavelength $K\alpha$ of copper ($\lambda=1.542\text{\AA}$). All the data were collected in the domain $10^\circ < 2\theta < 80^\circ$ with a step of 0.02° . The characterizations by infrared spectroscopy were carried out using the Perkin Elmer Spectrum type (Version 10.4.00). The same specimens, in the form of pellets, were examined under a scanning electron microscope SEM of type Hitachi S3400N then a UV- Vis – diffuse reflectance spectrometer of type JASCO apparatus. In addition, the measurements of the magnetic susceptibility of these samples were carried out by using the superconducting quantum interference magnetometer (SQUID). Finally, the electrical conductivity measurements were carried out using the classical two points method in the temperature range $425 - 800^\circ\text{C}$; The details of the electric conductivity measurements are described elsewhere. [41].

RESULTS AND DISCUSSION

Fig. 1 presents all the diffractograms of the system $\text{Bi}_{1.5-x}\text{M}_x\text{Sb}_{1.5-x}\text{M}'_x\text{ZnO}_7$ ($\text{M} = \text{Fe}$; $\text{M}' = \text{Fe, Cr}$) ($x=0$; 0.10 ; 0.15). Three limited solid solutions were obtained from

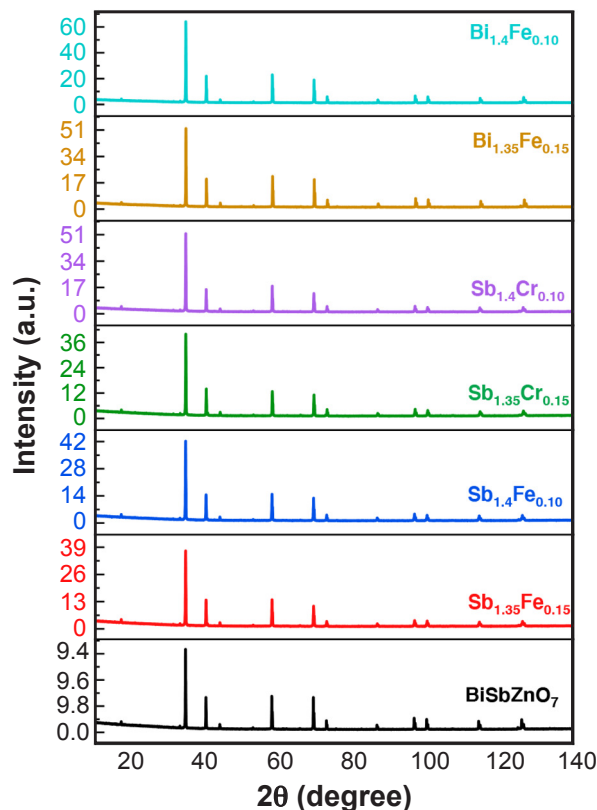


Figure 1: XRD patterns for the limited solid solution in the pyrochlore system according to formula $\text{Bi}_{1.5-x}\text{M}_x\text{Sb}_{1.5-x}\text{M}'_x\text{ZnO}_7$ ($\text{M} = \text{M}' \text{Fe} [\text{BiM}]; = \text{Fe, Cr} [\text{SbM}']$) ($x=0$; 0.10 ; 0.15).

formula $\text{Bi}_{1.5-x}\text{Fe}_x\text{Sb}_{1.5-x}\text{ZnO}_7$ [BiFe], $\text{Bi}_{1.5-x}\text{Sb}_x\text{Fe}_{1.5-x}\text{ZnO}_7$ [SbFe], and $\text{Bi}_{1.5-x}\text{Sb}_{1.5-x}\text{Cr}_x\text{ZnO}_7$ [SbCr]. All peaks are indexed in a face-centered cubic lattice (space group $\text{Fd}3\text{m}$), which are phases isotype to the basic compound $\text{Bi}_{1.5}\text{Sb}_{1.5}\text{ZnO}_7$ [7].

The refinement of the lattice parameters was carried out by the Rietveld method in the profile matching mode. Fig. 2 shows the evolution of the lattice parameter calculated for each system. The computed values of the lattice parameter, illustrate a regular decrease in the difference of the ionic radii of antimony ($R_{\text{VI}}=0.61\text{\AA}$), iron ($R_{\text{VI}}=0.55\text{\AA}$), chromium ($R_{\text{VI}}=0.55\text{\AA}$), bismuth ($R_{\text{VIII}}=1.17\text{\AA}$) and iron ($R_{\text{VIII}}=0.92\text{\AA}$) [42]. On the other hand, Scherrer's equation [43] was used to calculate the dimensions of the crystallites from the contribution of the size effect to the half-width of peaks. Indeed, the sizes in the interval range ($37.2 - 55.8 \text{ nm}$), depend upon the synthesis method, the diffusion during the sintering, and the substitution rate (x). Table 1 summarizes the calculated dimensions as well as values of gap energy and magnetic susceptibility parameters which will be discussed later on in the text. One can notice that the substitution in the "A" site keeps the same value; however, that in site "B" increases the average grain size with the same value for both iron and chromium.

The pyrochlore phase with the formula $\text{Bi}_{1.5}\text{Sb}_{1.5}\text{ZnO}_7$ was further refined according to XRD data. The ideal pyrochlore structure (space group $\text{Fd}-3\text{m}$) was used as a starting model [11]. The best agreement between experimental and

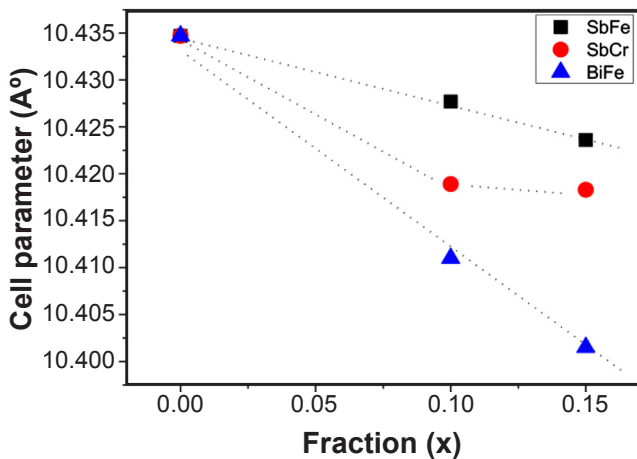


Figure 2: Variation of the lattice parameter of pyrochlore system $\text{Bi}_{1.5-x}\text{M}_x\text{Sb}_{1.5-x}\text{M}'_x\text{ZnO}_7$ ($\text{M}=\text{Fe}$ [BiM] $\text{M}'=\text{Fe, Cr}$ [SbM]) ($x=0.10; 0.15$).

calculated data was obtained for the disordered pyrochlore model. The results of the experimental composition refinement by this method are in satisfactory agreement with the assumed theoretical ones. The experimental, calculated, and difference diffractograms of $(\text{Bi}_{1.5}\text{Zn}_{0.5})(\text{Sb}_{1.5}\text{Zn}_{0.5})\text{O}_7$ are shown in Fig. 3. A characteristic result of the structure refinement, is the displacement of bismuth atoms from the highly symmetric positions 16d down to the 96g ones and the disordering of the oxygen crystallographic position to the filled 48f and deficient 32e. The zinc metal cations (Zn^{2+}) partially occupy the 96g and 16b positions with a percentage of 25% in each crystallographic site. This atomic distribution corresponds exactly to the calculated stoichiometric formula $(\text{Bi}_{1.5}\text{Zn}_{0.5})(\text{Sb}_{1.5}\text{Zn}_{0.5})\text{O}_7$. Tables 2 & 3 present the results of refining the pyrochlore structure for the composition calculated by the Rietveld method in the space group $\text{Fd-}3\text{m}$ ($N^\circ 227$). Fig. 4 gives the descriptions of the crystal structures by showing the location of the two sites “A” and “B” as well as the two types of oxygen. Table 4 yields some bond lengths in both sites. The refinement of the structure shows that the “B” site is formed by the two cations Sb^{5+} and Zn^{2+} forming a B-O6 octahedron with a bond length equal to 1.990(2) Å. Individual interatomic distances in the A-O8 polyhedron vary from 2.28 to 2.96 Å. The ion distribution model in the structure is similar to those described

elsewhere for pyrochlores in $\text{Bi}_{1.5}\text{Zn}_{0.92}\text{Nb}_{1.5}\text{O}_{6.92}$ systems [8]. The pyrochlore unit cell parameter is 10.44425(3) Å. This value is less than the one for Zn-containing pyrochlore i.e. 10.5616(1) Å based on bismuth niobate [8] and subsequently, the values determined for cobalt pyrochlores based on bismuth antimonate i.e. 10.44896(2) Å [11]. The lattice parameter is directly related to the value of the ionic radii of the cations constituting the crystalline structure.

Fig. 5 presents the different surface morphologies of the phases from the photographs taken on the pellets. The micrographs of $\text{Bi}_{1.5}\text{Sb}_{1.5-x}\text{Fe}_x\text{ZnO}_7$ and $\text{Bi}_{1.5}\text{Sb}_{1.5-x}\text{Cr}_x\text{ZnO}_7$ ($x=0.1$ and $x=0.15$) show relatively dense phases with a particle size that changes slightly depending on the substitution rate (x), the size of the ionic radii and probably the effect of the diffusion rate of the ionic species during the growth of the grains while sintering. In the case of $\text{Bi}_{1.5-x}\text{Fe}_x\text{Sb}_{1.5}\text{ZnO}_7$ ($x=0.10$ and $x=0.15$), one can observe a more porous surface with an irregular lump-like morphology with a spherical shape of its grains despite the remarkable difference in the size of the ions [$\text{R}_{\text{Bi}(\text{VIII})}=1.17\text{Å}$; $\text{R}_{\text{Fe}(\text{VIII})}=0.92\text{Å}$]. The phases resulting from the substitution of Bi by Fe permit the formation of crystallites of smaller size leading to a morphology composed of them, which tends to settle along the same plane. Figure 6 displays the EDS analysis data of some synthesized samples. Indeed, all the metal cations Bi, Sb, Zn, Fe, and Cr are present. Table 5 summarizes the values expressed in mass percentage of all the cations forming the synthesized compounds.

The pyrochlore $\text{A}_2\text{B}_2\text{O}_7$ phases have already been the subject of such analyses and the frequencies of the vibrations of the infrared lattice of certain compounds have been studied elsewhere [44, 45]. Indeed, the interpretation of the FTIR spectra can provide further information on the nature of possible order defects in the pyrochlores [46]. In our case, as shown in Fig. 7, the spectra display similarities where the absorption bands occurring in the range 400 - 2000 cm^{-1} , correspond to the same vibrational frequencies that are generally attributed to vibrations of metal ions in the crystal lattice [47]. The frequency of the strongest band is located at about 648 cm^{-1} and is attributed to the Zn–O stretching vibration in the ZnO_6 octahedron. Another weak band located at about 480 cm^{-1} appears from the Bi–O or Sb–O stretching vibration [48]. Moreover, two very weak vibration bands are observed in the 1000 and 1400 cm^{-1}

Table 1 - Crystallite dimensions, energy band gaps, effective magnetic moments, and colors for pyrochlore compounds.

| Compound | $\text{Bi}_{1.5}\text{Sb}_{1.5}\text{ZnO}_7$ | $\text{BiFe}_{0.10}$ | $\text{BiFe}_{0.15}$ | $\text{SbFe}_{0.10}$ | $\text{SbFe}_{0.15}$ | $\text{SbCr}_{0.10}$ | $\text{SbCr}_{0.15}$ |
|--|--|----------------------|----------------------|----------------------|----------------------|----------------------|----------------------|
| Color | White | Yellow | Yellow | Yellow | Yellow | Green | Green |
| D (nm) | 37.2 | 37.2 | 37.2 | 55.8 | 55.8 | 55.8 | 55.8 |
| Gap Energy (eV) | 3.36 | 2.92 | 2.90 | 2.72 | 2.66 | 2.94 | 2.80 |
| μ_{eff} (μBohr)/ M^{3+} | 0 | 5.78 | 5.19 | 5.31 | 5.73 | 3.98 | 3.66 |

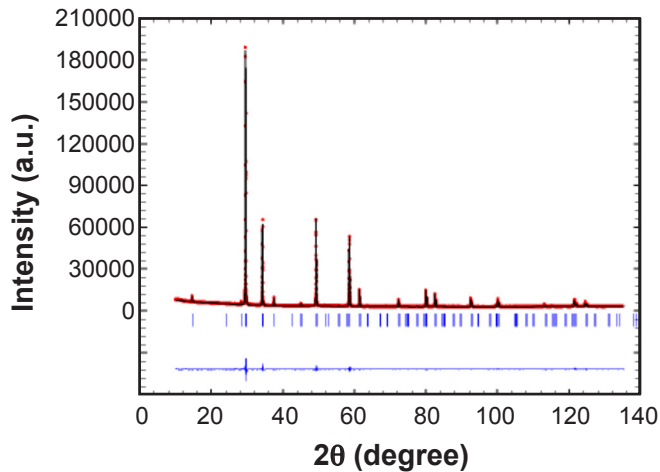


Figure 3: Theoretical, calculated, and difference XRD powder diffraction of $\text{Bi}_{1.5}\text{Sb}_{1.5}\text{ZnO}_7$ pyrochlore structure.

Table 2 - Rietveld refinement results.

| ZnGlobal formula | $\text{Bi}_{12}\text{Sb}_{12}\text{Zn}_8\text{O}_{56}$ |
|---------------------|--|
| Formula weight | 5387.77 |
| Crystalline system | Cubic |
| Space group | $\text{Fd}\bar{3}\text{m}(\text{N}^\circ 227)$ |
| Cell parameter | 10.44425(3) |
| Cell volume | 1139.282(5) |
| Volume mass | 7.853g/cm ³ |
| Reflection number | 79 |
| Refinement number | 102 |
| Zero point(2θ°) | 0.01988 |
| Sycos | 0 |
| Function profile | Pseudo-Voigt |
| | U:0.02481 |
| Half width | V:-0.01731 |
| | W:0.00879 |
| | 0.12203(0) |
| Asymmetry parameter | 0.05712(0) |
| | 0.00000 |
| | 0.00000 |
| R_{wp} | 2.86 |
| R_{p} | 2.03 |
| R_{exp} | 1.58 |
| R_{Bragg} | 1.92 |
| R_{f} | 2.14 |

Table 4 - Selected bond lengths (Å) and angles (°).

| Bond type | Length (Å) |
|-----------------|-----------------------|
| (Sb2/Zn2)-O1 | $1.990(2) \times 6$ |
| | $2.791(3) \times 2$ |
| (Bi1/Zn1)-O1 | $2.496(3) \times 2$ |
| | 2.289(4) |
| | 2.964(3) |
| A-(Bi1/Zn1)-O2 | 1.934(18) |
| Angle type | Angle (°) |
| | $180.00(19) \times 3$ |
| | $93.43(15) \times 6$ |
| O1-Sb2-O1 | $86.57(8) \times 6$ |

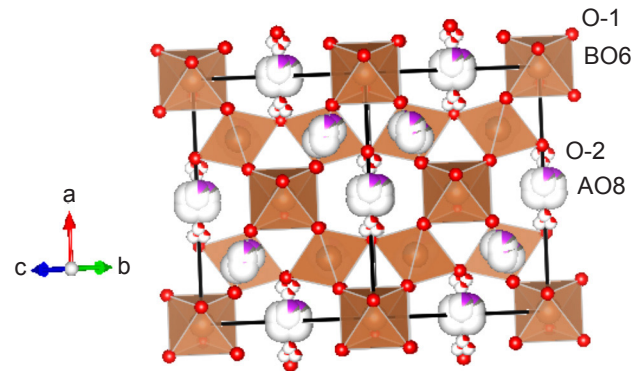


Figure 4: $(\text{Bi}_{1.5}\text{Zn}_{0.5})(\text{Sb}_{1.5}\text{Zn}_{0.5})\text{O}_7$ cubic pyrochlore structure.

domains and suggest that these modes are an indicator of the additional structural complexity of this network.

Fig. 8 exhibits the reflectance spectra of our synthesized samples. It is well shown that the basic compound $\text{Bi}_{1.5}\text{Sb}_{1.5}\text{ZnO}_7$ absorbs radiation in the UV range. The absorbance increases drastically beyond 400 nm. The other compositions can shift the absorbance in the visible range between 500 and 400 nm for the two solid solutions (BiFe, SbFe, and SbCr). The UV-Vis spectrum can be used to calculate the band gaps of semiconductor material. The Kubelka-Munk (K-M) formalism is thus used to analyze the reflectance spectrum. The K-M Function $F(R)$ is given by Eq.1 [49, 50].

$$F(R) = \frac{(1-R)^2}{2R} \quad (\text{A})$$

Therefore, from Eq.A, the familiar K-M conversion follows straightforwardly. It is thus given by Eq. B

Table 3 - Atomic positions and site occupation.

| Atom | Position | x | Y | Z | Biso [Å ²] | Occupation |
|-------|----------|------------|------------|------------|------------------------|------------|
| Bi(1) | 96g | 0.4789(3) | 0.5174(2) | 0.5174(2) | 0.09999(13) | 0.125 |
| Zn(1) | 96g | 0.4789(3) | 0.5174(2) | 0.5174(2) | 0.09999(13) | 0.04166 |
| Sb(2) | 16c | 0.00000(0) | 0.00000(0) | 0.00000(0) | 0.03076(0) | 0.75 |
| Zn(2) | 16c | 0.00000(0) | 0.00000(0) | 0.00000(0) | 0.03076(0) | 0.25 |
| O(1) | 48f | 0.3212(3) | 0.12500(0) | 0.12500(0) | 1.53(11) | 1 |
| O(2) | 32e | 0.3901(17) | 0.3901(17) | 0.3901(17) | 1.53(11) | 0.25 |

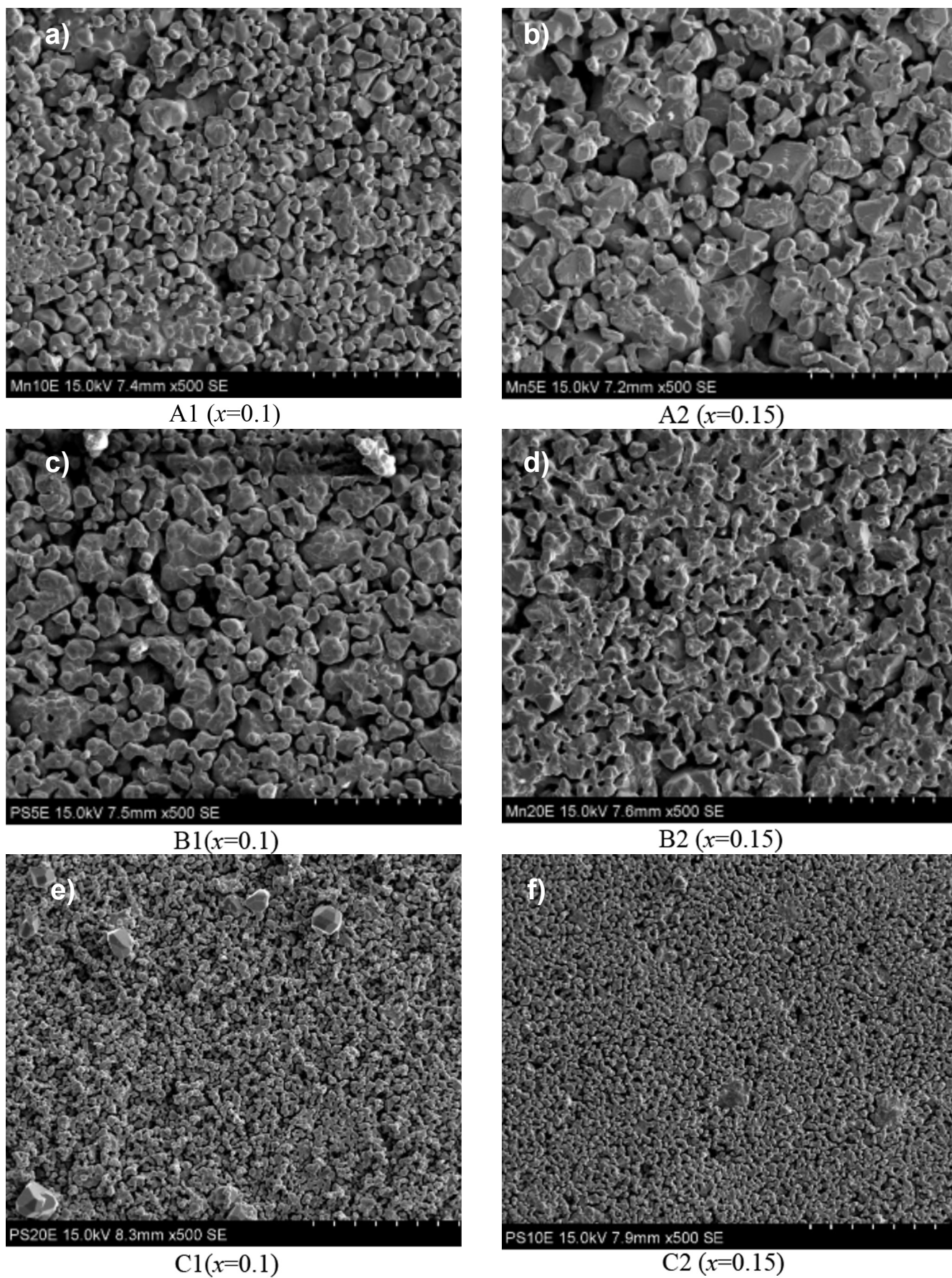


Figure 5: SEM phase micrographs: (A) $\text{Bi}_{1.5}\text{Sb}_{1.5-x}\text{Fe}_x\text{ZnO}_7$; (B) $\text{Bi}_{1.5}\text{Sb}_{1.5-x}\text{Cr}_x\text{ZnO}_7$ and (C) $\text{Bi}_{1.5-x}\text{Fe}_x\text{Sb}_{1.5}\text{ZnO}_7$ ($x=0.10$; $x=0.15$).

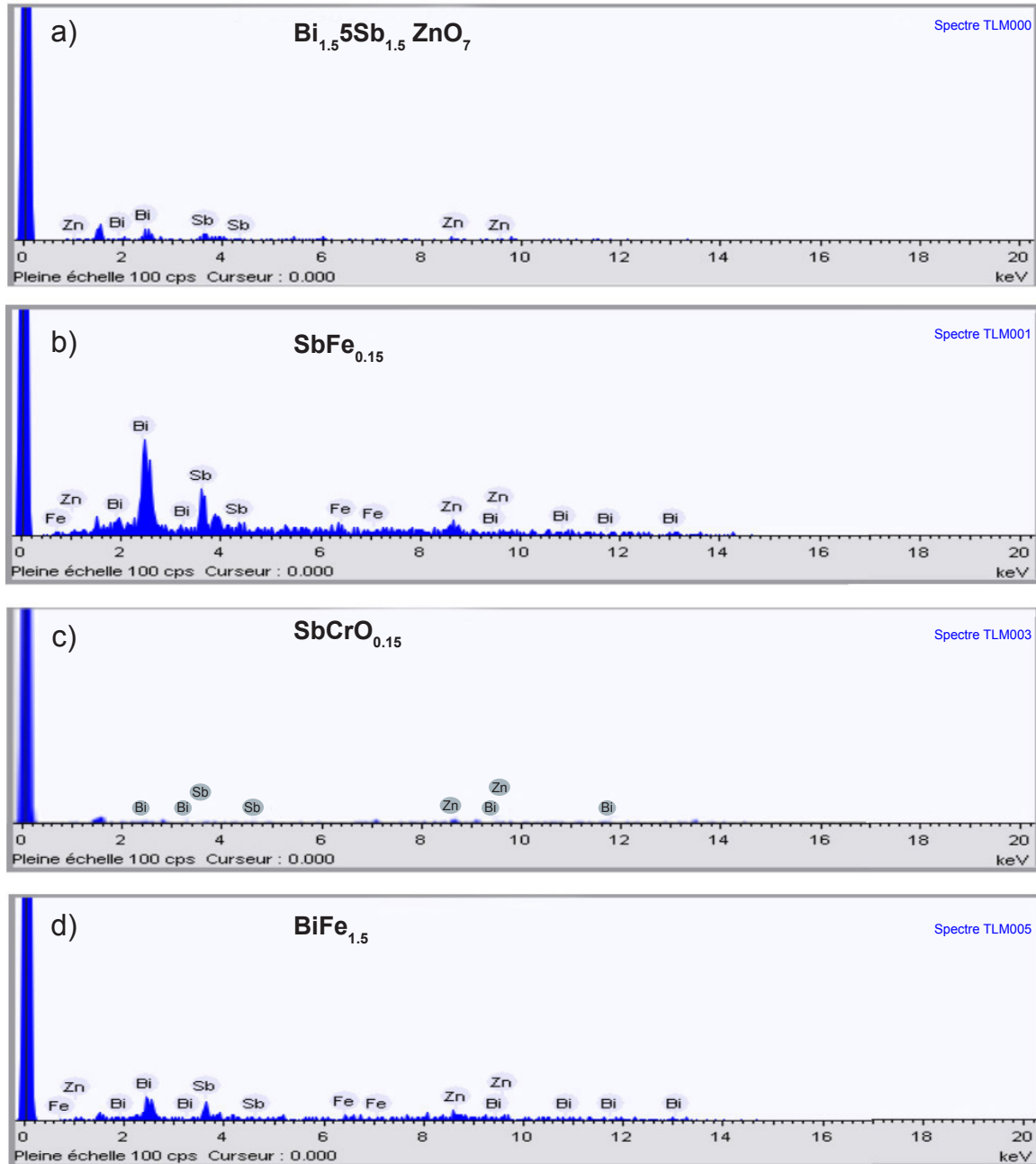


Figure 6: EDS analysis data of some synthesized compounds.

Table 5. EDS analysis data.

| Sample | Bi | Zn | Sb | Cr | Fe |
|--|------|------|------|-----|-----|
| $\text{Bi}_{1.5}\text{Sb}_{1.5}\text{ZnO}_7$ | 58.2 | 16.2 | 25.6 | - | - |
| $\text{SbFe}_{0.15}$ | 56.4 | 5.1 | 35.5 | - | 2.9 |
| $\text{SbCrO}_{0.15}$ | 68.1 | 5.1 | 26.3 | 0.5 | - |
| $\text{BiFe}_{1.5}$ | 50.7 | 6.1 | 40.5 | - | 2.7 |

$$\frac{K}{S} = F(R) = \frac{(1-R)^2}{2R} \quad (\text{B})$$

where (R) is the absolute reflectance of the sample. In this

formula, the molar coefficient “k” identifies $(1-R)^2$, while the scattering factor “s” identifies $2R$. The K-M transform of the measured spectroscopic observable is roughly proportional to the absorption coefficient and hence is approximately proportional to the concentration given by Eq. C. On the other hand, the optical band gap values are estimated from the Tauc relation. The Kubelka-Munk function $F(R)$ is generally applied to convert the diffused reflectance (R) and consequently to calculate the optical reflectance data according to Eq.D.

$$\alpha = F(R) = \frac{(1-R)^2}{2R} \quad (\text{C})$$

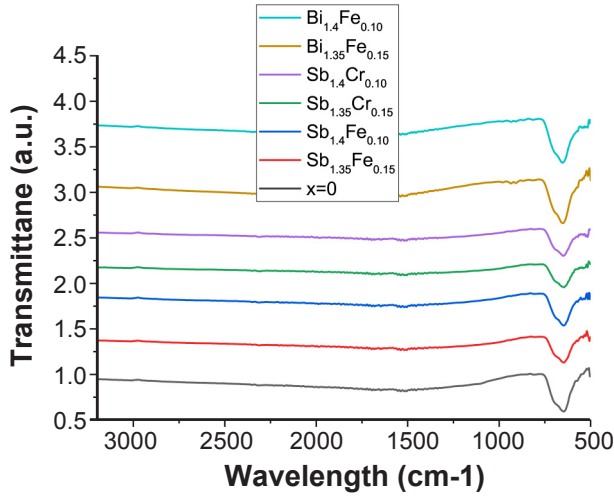


Figure 7: FTIR spectra of the $\text{Bi}_{1.5-x}\text{M}_x\text{Sb}_{1.5-x}\text{M}'\text{ZnO}_7$ ($\text{M} = \text{Fe}$ [BiM]; $\text{M}' = \text{Fe}, \text{Cr}$ [SbM']) compounds ($x=0; 0.10; 0.15$).

where (α) is the absorption coefficient and $F(R)$ is the Kubelka-Munk function. Thus, the Tauc relation can be written as,

$$F(R).h\nu = A(h\nu - E_g)^n \quad (\text{D})$$

where $n=2$ and $1/2$ represent the allowed indirect and direct transitions respectively. So, in this way, the indirect and direct band gaps can be assessed. The Tauc plot $[F(R).h\nu]^2$ versus $(h\nu)$ for a given compound, can be given. The plots of SbFe, SbCr, and BiFe compounds with different substitution rates are shown in Fig. 8. In consequence, the extrapolation of the linear regions in the plots i.e. $F(R).h\nu)^2 = 0$, yields the direct energy band gaps. Their values for the different pyrochlore compositions are listed in Table 1.

It is clear from this table that the absorbance shifts towards the visible and contributes to the Energy Band Gap values of the synthesized samples.

Similarly, to the pyrochlore cobalt oxides [41], our newly synthesized bismuth-based pyrochlore compounds

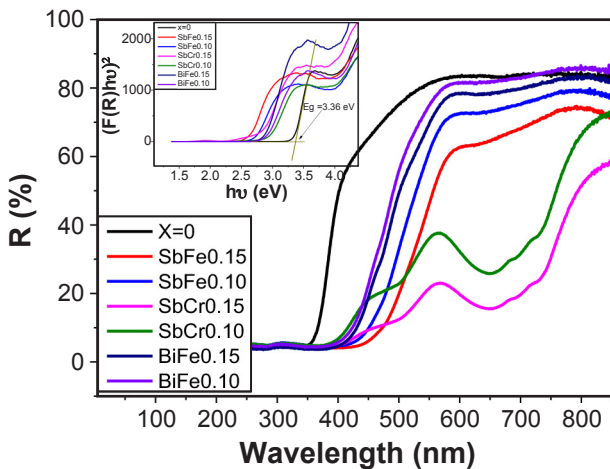


Figure 8: UV-Vis-DRS reflection $R(\%)$ spectra of the compounds. (Inset: Plots of $[F(R).h\nu]^2$ vs. $(h\nu)$ for some different compounds.

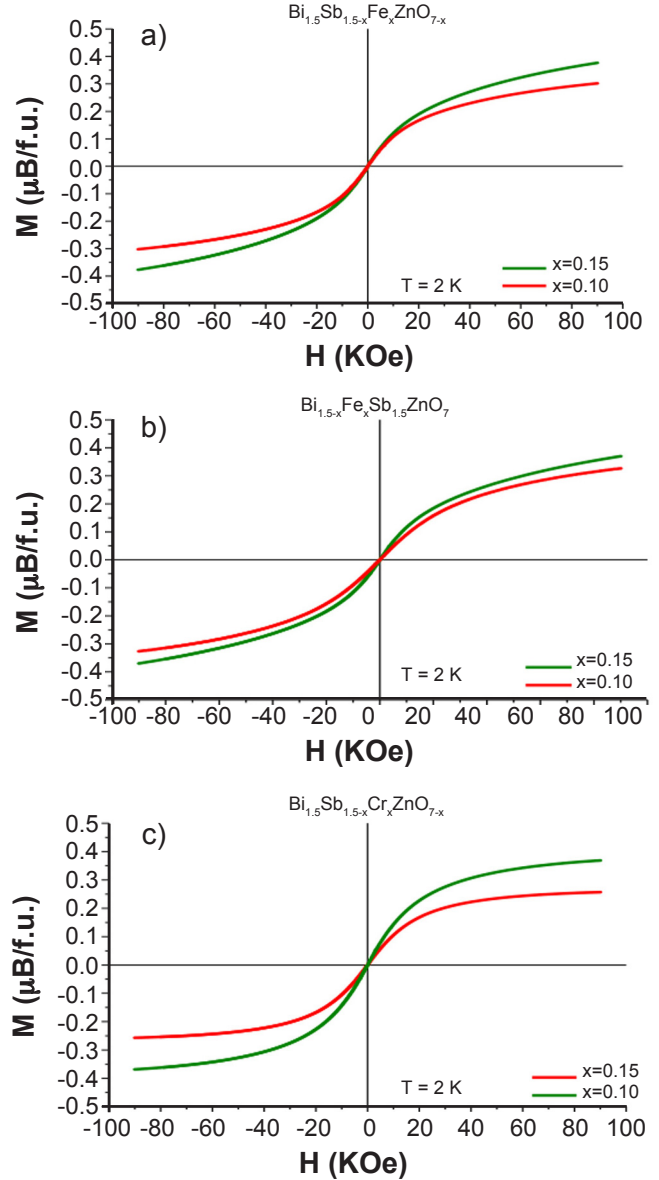


Figure 9: Magnetization versus Applied magnetic field of $\text{Bi}_{1.5-x}\text{M}_x\text{Sb}_{1.5-x}\text{M}'\text{ZnO}_{7-\delta}$ ($\text{M} = \text{Fe}$ [BiM]; $\text{M}' = \text{Fe}, \text{Cr}$ [SbM']) with substitution rates 0.10 and 0.15 (unit kOe).

exhibit the best physical properties which are the magnetic susceptibility and the electric conductivity.

The magnetic data obtained for the compounds indicate that the magnetization evolves according to the maximum magnetic field applied (i.e. 9.0 T) at absolute temperature 2.0 K. In such experimental conditions, the saturation cannot be reached. This behavior is similar for both pyrochlore compounds displayed in Fig.9. The field dependence of the magnetization confirms that the sample is overall naturally paramagnetic. The temperature dependence of the inverse magnetic susceptibility is shown in Fig. 10. Above 100K, the inverse magnetic susceptibility is linear and fits satisfactorily to the modified CW law. The observed effective magnetic moments μ_{eff} , calculated from the slopes of these linear fits, are listed in Table 1. The values found for our compounds are due to the contribution of the magnetic moments arising from

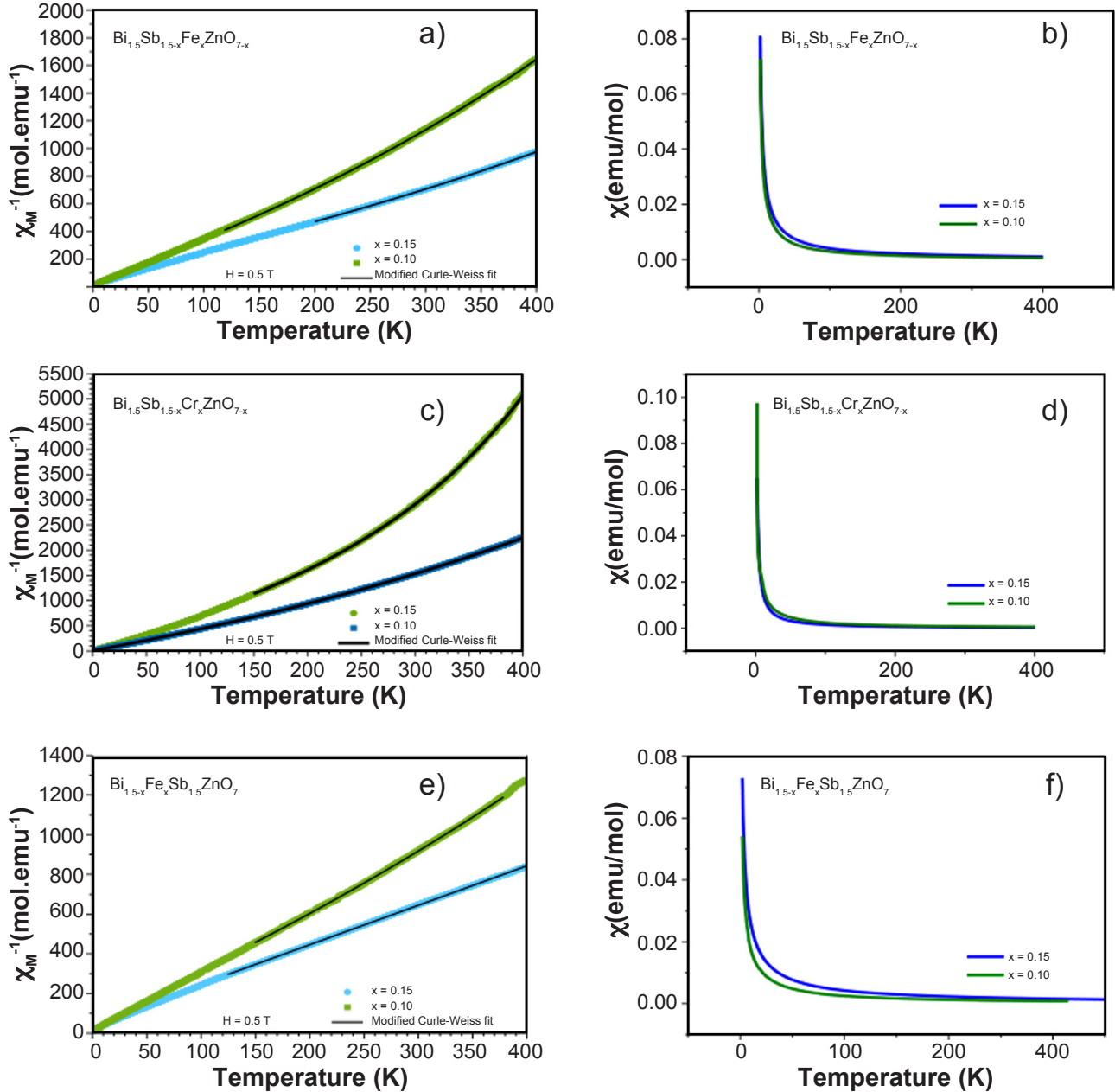


Figure 10: Susceptibility versus temperature of $\text{Bi}_{1.5-x}\text{M}_x\text{Sb}_{1.5-x}\text{M}'_x\text{ZnO}_{7-\delta}$ ($\text{M} = \text{Fe}$ [BiM]; $\text{M}' = \text{Fe}, \text{Cr}$ [SbM']) with substitution rates 0.10 and 0.15 (unit KOe).

the iron and chromium ions. These values are in concordance with those usually found in transition metal spin-free configurations [51]. The four observed effective magnetic moments of iron ranging from 5.19 to 5.78 μ_B and those two observed of chromium (3.66; 3.98 μ_B) indicate that the spin-only values expected for $\text{Fe}^{3+}(3d^5, \text{high spin } t_{2g}^3 e_g^2)$ i.e. $\mu_{\text{obs}} = 5.6 - 6.1 \mu_B$ [52] and for $\text{Cr}^{3+}(3d^3, \text{high spin } t_{2g}^3)$ i.e. $\mu_{\text{obs}} = 3.7 - 3.9 \mu_B$ [52].

It is well known that the electrical conductivity of any material describes its transport property ensured by its electronic/ionic species being involved. It increases naturally with the increase in concentration and is very sensitive to the variation of the temperature. The Arrhenius relation i.e. $\sigma = \sigma_0 \cdot \exp[-E_a/(K_B T)]$ is well known to describe

the temperature dependence of physical parameters such as electric conductivity, dielectric relaxation, ...etc. So by applying the decimal logarithm to electric conductivity versus the inverse temperature, one can find the values of the activation energy (E_a) and the reference conductivity (σ_0). The electrical conductivity obeying the Arrhenius behavior may be described by Eq. E

$$\log(\sigma) = \log(\sigma_0) - E_a/(K_B T) \quad (\text{E})$$

where σ_0 represents a pre-exponential factor, E_a is the activation energy, K_B Boltzmann constant, and T absolute temperature. Fig. 11 gives the temperature dependence of $\log(\sigma)$ for $\text{SbFe}_{0.15}$ and $\text{SbCr}_{0.15}$ pyrochlore compounds

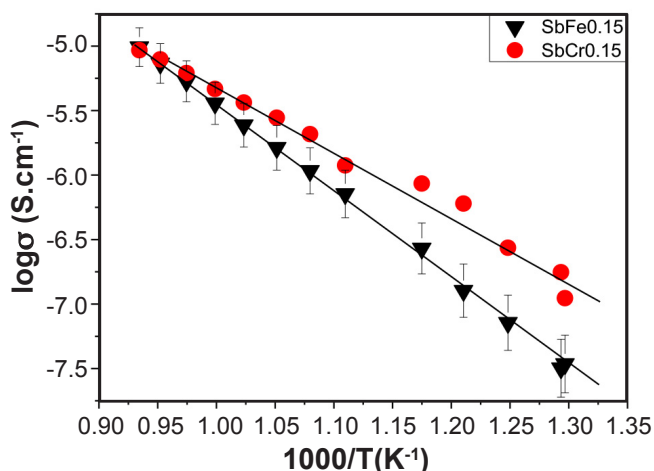


Figure 11: Log (σ) vs. ($1/T$) of SbFe and SbCr at the same substitution rate of 0.15.

with the same substitution rate of 0.15. The substitution of the antimony cation (Sb^{5+}) by those of iron (Fe^{3+}) and chromium (Cr^{3+}), induces oxygen deficiency in the formulae of the limited solid solutions. These formulae can therefore be written simply as follows: $\text{Bi}_{1.35}^{3+}\text{Sb}_{0.15}^{5+}\text{Fe}_{0.15}^{3+}\text{Zn}_{0.15}^{2+}\text{O}_{7-\delta}^{2-}$ and $\text{Bi}_{1.35}^{3+}\text{Sb}_{0.15}^{5+}\text{Cr}_{0.15}^{3+}\text{Zn}_{0.15}^{2+}\text{O}_{7-\delta}^{2-}$. The value of oxygen deficit is thus estimated in the formulae at $\delta = 0.15$. The presence of oxygen deficiency in compounds makes it easier for both electronic and ionic conductivities. In the investigated temperature range of 425 - 800°C, the electronic conductivity data of $\text{SbCr}_{0.15}$ lie above those of $\text{SbFe}_{0.15}$. At higher temperatures, they exhibit almost the same values, while they become quite different from each other as the temperature decreases. Moreover, the function $\log(\sigma)$ vs. ($1/T$) yields a straight slope (E_a/K_B) from which the value of E_a can be deduced graphically. Thus, the values of E_a are 1.35 eV and 0.97 eV for the $\text{SbFe}_{0.15}$ and $\text{SbCr}_{0.15}$ respectively. These interesting results reveal the semi-conducting behavior of these newly synthesized compounds. This electrical behavior is similar to the electrical conductivity of the solid solution of pyrochlore type with formula $\text{Bi}_{1.56-x}\text{Ca}_x\text{Sb}_{1.48}\text{Co}_{0.96}\text{O}_7$ recently synthesized [41].

CONCLUSION

In the present investigation, we have explored the partial substitution of Bismuth by Iron and Antimony by Iron and Chromium in the pyrochlore material $\text{Bi}_{1.5}\text{Sb}_{1.5}\text{ZnO}_7$. The substitution limit was found equal to $x=0.15$ for the three types of substitutions. XRD analysis revealed a pyrochlore structure for all the compositions. The lattice parameters evolve according to the ionic radii. The Scherrer equation showed grain size in the range of 37.2 - 55.8 nm. The micrographs of compounds show relatively dense phases with a particle size that changes slightly depending on the substitution rate (x). UV-Visible diffuse makes evidence of the absorbance shift towards the visible that contributes to the Energy Band Gap level. The lowest value is given by

the compound $\text{Bi}_{1.35}\text{Fe}_{0.15}\text{Sb}_{1.5}\text{ZnO}_7$ ($\text{BiFe}_{0.15}$). The values of the activation energy (E_a) are 1.35 eV and 0.97 eV for the $\text{SbFe}_{0.15}$ and $\text{SbCr}_{0.15}$ compounds respectively. These results reveal the semiconducting behavior of these pyrochlore materials. The magnetic measurements show the magnetic behavior of the samples. The calculated magnetic susceptibilities reveal values comprised between 3.66 and 5.78 μ_{Bohr} in concordance with those usually found in transition metal spin-free configurations.

ACKNOWLEDGEMENTS

We would like to thank Dr Olivier Mentré, Research Director at CNRS, for his fruitful discussions and technical assistance in carrying out magnetism analyses and electrical measurements in his laboratory at the Lille National School of Chemistry (ENSCL-BP). 9010).

REFERENCES

- [1] Gaines RV, Skinner HCW, Foord EE, Mason B, Rosenzweig A. Dana's New Mineralogy. 8th ed. New York: Wiley; 1997. p. 341–52. doi:10.1180/002646198547693.
- [2] Sellami M, Caignaert V, Hamdad M, Bekka A, Bettahar N. Synthesis and characterization of the pyrochlore solid solution $\text{Bi}_{1.5}\text{Sb}_{1.5}\text{Cu}_{1-x}\text{Mn}_x\text{O}_7$. *J Alloys Compd.* 2009;**482**(1-2):13-8. doi:10.1016/j.jallcom.2009.04.017.
- [3] Sellami M, Bekka A, Bettahar N. Synthèse et résolution structurale par la méthode de Rietveld d'un nouveau composé de type pyrochlore de formule $(\text{Bi}_{1.524}\text{Cu}_{0.476})(\text{Sb}_{1.524}\text{Cu}_{0.476})\text{O}_7+\text{d}$. *C R Chim.* 2005;**8**:1129-34. doi:10.1016/j.crci.2005.01.005.
- [4] Kennedy BJ. Structural trends in pyrochlore-type oxides. *Physica B Condens Matter.* 1997;**241-243**:303-10. doi:10.1016/s0921-4526(97)00570-x.
- [5] Xiuli C, Dandan M, Guisheng H, Gaofeng L, Huanfu Z. Structure and dielectric properties of a novel defect pyrochlore BiFeNbO ceramic. *J Mater Sci Mater Electron.* 2016;**27**(8):8619-22. doi:10.1007/s10854-016-4881-y.
- [6] Clayton J, Takamura H, Metz R, Tuller HL, Wuensch BJ. The Electrical and Defect Properties of $\text{Bi}_3\text{Zn}_2\text{Sb}_3\text{O}_{14}$ Pyrochlore: A Grain-Boundary Phase in ZnO-Based Varistors. *J Electroceram.* 2001;**7**:113-20. doi:10.1023/b.0000027951.41051.11.
- [7] Peiteado M, De La Rubia MA, Fernández JF, Caballero AC. Thermal evolution of $\text{ZnO-Bi}_2\text{O}_3\text{-Sb}_2\text{O}_3$ system in the region of interest for varistors. *J Mater Sci.* 2006;**41**:2319-25. doi:10.1007/s10853-006-7168-5.
- [8] Levin I, Amos TG, Nino JC, Vanderah TA, Randall CA, Lanagan MT. Structural study of an unusual cubic pyrochlore $\text{Bi}_{1.5}\text{Zn}_{0.92}\text{Nb}_{1.5}\text{O}_{6.92}$. *J Solid State Chem.* 2002;**168**(1):69-75. doi:10.1006/jssc.2002.9681.
- [9] Nino JC, Lanagan MT, Randall CA. Dielectric relaxation in $\text{Bi}_2\text{O}_3\text{-ZnO-Nb}_2\text{O}_5$ cubic pyrochlore. *J Appl Phys.* 2001;**89**(8):4512. doi:10.1063/1.1357468.
- [10] Sellami M, Caignaert V, Hamdad M, Belarbi A, Sari IM, Bahmani A, Bettahar N. Synthesis and characterization

- of the new pyrochlore $\text{Bi}_{1.5}\text{Sb}_{1.5-x}\text{Nb}_x\text{MnO}_7$ solid solution. *C R Chim.* 2011;**14**(10):887-90. doi:10.1016/j.crci.2011.05.010.
- [11] Sellami M, Bekka A, Bettahar N, Caignaert V, Nguyen N. Crystallographic, magnetic and electric studies of a new pyrochlore-like structure $(\text{Bi}_{1.56}\text{Co}_{0.44})(\text{Sb}_{1.48}\text{Co}_{0.52})\text{O}_7$ compound. *C R Chim.* 2009;**12**(1-2):276-83. doi:10.1016/j.crci.2008.01.002.
- [12] Sellami M, Caignaert V, Bekka A, Bettahar N. Synthesis and characterization of the pyrochlore $\text{Bi}_{1.56}\text{Sb}_{1.48-x}\text{Nb}_x\text{Co}_{0.96}\text{O}_7$ solid solution. *J Alloys Compd.* 2010;**493**:91-4. doi:10.1016/j.jallcom.2009.12.059.
- [13] Golden R, Mueller K, Opila E. Thermochemical stability of $\text{Y}_2\text{Si}_2\text{O}_7$ in high-temperature water vapor. *J Am Ceram Soc.* 2020;**103**(8):4517-35. doi:10.1111/jace.17114.
- [14] Cava RJ, Peck WF Jr, Krajewski JJ. Pyrochlore based oxides with high dielectric constant and low temperature coefficient. *J Appl Phys.* 1995;**78**(12):7231-3. doi:10.1063/1.360434.
- [15] Rao PP, Nair KR, Koshy P, Vaidyan VK. Microwave dielectric properties of new pyrochlore type oxides: $\text{Pb}_3\text{R}_3\text{Ti}_7\text{Nb}_2\text{O}_{26.5}$ ($\text{R} = \text{Y}, \text{Pr}, \text{Nd}, \text{Gd}$ or Dy). *Mater Sci Eng B.* 2006;**128**(1-3):184-7. doi:10.1016/j.mseb.2005.11.031.
- [16] Subramanian MA, Sleight AW. New pyrochlores of the type $(\text{CdBi})(\text{M}, \text{M}')_2\text{O}_7$. *Mater Res Bull.* 1986;**21**(6):727-32. doi:10.1016/0025-5408(86)90152-2.
- [17] Wuensch BJ, Eberman KW, Heremans C, Ku EM, Onnerud P, Yeo EM, Haile SM, Stalick JK, Jorgensen JD. Connection between oxygen-ion conductivity of pyrochlore fuel-cell materials and structural change with composition and temperature. *Solid State Ionics.* 2000;**129**:111-33. doi:10.1016/S0167-2738(99)00320-3.
- [18] Avdeev M, Haas MK, Jorgensen JD, Cava RJ. Static disorder from lone-pair electrons in pyrochlores. *J Solid State Chem.* 2002;**169**(1):24-34. doi:10.1016/S0022-4596(02)00007-5.
- [19] Yonezawa S, Muraoka Y, Matsushita Y, Hiroi Z. New pyrochlore oxide superconductor RbOs_2O_6 . *J Phys Soc Jpn.* 2004;**73**:819-21. doi:10.1143/jpsj.73.819.
- [20] Beck E, Ehmann A, Krutzsch B, Kemmler-Sack S, Khan HR, Raub CJ. Investigation of superconductivity and physical properties of some spinel-, perovskite- and pyrochlore-type oxides. *J Less Common Met.* 1989;**147**(L17). doi:10.1016/0022-5088(89)90202-6.
- [21] Mayer-Von Kuerthy G, Wischert W, Kiemel R, Kemmler-Sack S. System $\text{Bi}_{2-x}\text{Pb}_x\text{Pt}_2-x\text{Ru}_x\text{O}_7-z$: A pyrochlore series with a metal-insulator transition. *J Solid State Chem.* 1989;**79**(1):34-45. doi:10.1016/0022-4596(89)90247-8.
- [22] Yonezawa S, Muraoka Y, Matsushita Y, Hiroi Z. New pyrochlore oxide superconductor RbOs_2O_6 . *J Phys Soc Jpn.* 2004;**73**:819-21. doi:10.1143/jpsj.73.819.
- [23] Hiroi Z, Yonezawa S, Muramatsu T, Yamaura JI, Muraoka Y. Specific heat of the β -pyrochlore oxide superconductors CsOs_2O_6 and RbOs_2O_6 . *J Phys Soc Jpn.* 2005;**74**:1255-62. doi:10.1143/jpsj.74.1255.
- [24] Calage Y, Pannetier J. Electric field gradients in pyrochlore compounds. *J Phys Chem Solids.* 1977;**38**(7):711-8. doi:10.1016/0022-3697(77)90062-2.
- [25] Anderson JB, McKenzie G. Chemistry of Pyrochlore Structures: A Handbook. Wiley-Interscience; 2000. p. 45-69. doi:10.1111/jace.18566.
- [26] Yoshimura M, Okazaki M. Study on Phase Diagram and Structure of Bi_2O_3 - PbO - Nb_2O_5 System. *J Am Ceram Soc.* 1979;**62**:234-9. doi:10.1111/j.1151-2916.1979.tb09752.x.
- [27] Swinnea JS, Steinfink H. Structure of $\text{Pb}_2\text{Ru}_2\text{O}_7$ Pyrochlore Oxide. *J Solid State Chem.* 1981;**36**:77-82. doi:10.1016/0022-4596(81)90136-6.
- [28] Ruiz MI, Gallego H. Magnetic Susceptibility of $\text{B}_2\text{ZrRu}_0.5\text{Fe}_0.5\text{O}_7$ Pyrochlore-Type Compounds. *J Appl Phys.* 1995;**78**:3458. doi:10.1063/1.359742.
- [29] Sasaki S, Nishihara H, Fukase H, Ohya H. Electrical conductivity of pyrochlore-type oxides, $\text{Bi}_{2-x}\text{Sr}_x\text{Ru}_2\text{O}_{7-\delta}$. *J Solid State Chem.* 1987;**70**:299-307. doi:10.1016/0022-4596(87)90332-4.
- [30] Shevchenko IV, Gorshkov VT, Sviridov DS. Pyrochlore structure and its role in the radiation stability of ceramics for nuclear applications. *Russ Chem Rev.* 2003;**72**:39-58. doi:10.1070/rc2003v072n01abeh000707.
- [31] Cava RJ, Santoro A, Murphy DW. Phase transitions in oxide pyrochlores. *J Solid State Chem.* 1983;**49**:285-90. doi:10.1016/0022-4596(83)90325-9.
- [32] Sleight AW. Pyrochlore oxides: Crystal chemistry, structure, and physical properties. *Annu Rev Mater Sci.* 1979;**9**:101-23. doi:10.1146/annurev.ms.09.080179.000533.
- [33] Subramanian MA, Sleight AW. Ternary Rare Earth-Based Pyrochlore Oxides. *Mater Res Bull.* 1981;**16**:1555-63. doi:10.1016/0025-5408(81)90098-7.
- [34] Kanamori J. The theory of Pyrochlore compounds. *J Phys Chem Solids.* 1957;**8**:2-6. doi:10.1016/0022-3697(57)90163-3.
- [35] Gardner JS, Gingras MJ, Greedan JE. Pyrochlore antiferromagnets. *Rev Mod Phys.* 2010;**82**:53-107. doi:10.1103/revmodphys.82.53.
- [36] Schiffer P, Ramirez AP. Magnetic field effects on the pyrochlore structure. *Phys Rev Lett.* 1994;**73**:2500. doi:10.1103/physrevlett.73.2500.
- [37] Castro F, Ramos F, Freire F, Míguez J. Structural and magnetic characterization of $(\text{Nd}, \text{Y})\text{MnO}_3$ pyrochlores. *J Appl Phys.* 1999;**85**:5364-70. doi:10.1063/1.370418.
- [38] Gingras MJ, Gaulin BD, Cava RJ. Magnetic and electronic properties of pyrochlore oxides. *J Appl Phys.* 1998;**83**:6220. doi:10.1063/1.367501.
- [39] Rosenkranz S, Ramirez AP, Hayashi A, Cava RJ. Spin dynamics in geometrically frustrated pyrochlores. *Phys Rev B.* 2000;**62**:1419. doi:10.1103/physrevb.62.1419.
- [40] Ramirez AP, Hayashi A, Cava RJ. Geometrically frustrated magnetism in pyrochlores. *Phys Rev Lett.* 1994;**73**:1042. doi:10.1103/physrevlett.73.1042.
- [41] Hanawa M, Yonezawa S, Muraoka Y, Hiroi Z. Superconductivity in pyrochlore oxide $\text{Cd}_2\text{Re}_2\text{O}_7$. *Phys Rev Lett.* 2001;**87**:187001. doi:10.1103/physrevlett.87.187001.
- [42] Chapon LC, Bramwell ST. Spin-liquid state in the pyrochlore $\text{Nd}_2\text{Sn}_2\text{O}_7$. *Phys Rev Lett.* 2004;**93**:087201.

doi:10.1103/physrevlett.93.087201.

[43] Kermarrec E, Gauthier N, Castelnau A. Neutron scattering in pyrochlore oxides. *Phys Rev B*. 2015;**91**:1428. doi:10.1103/physrevb.91.1428.

[44] Takigawa M, Kubo M, Sasago Y. Pyrochlore antiferromagnet Nd₂Ir₂O₇. *J Phys Soc Jpn*. 2002;**71**:272. doi:10.1143/jpsj.71.272.

[45] Inagaki S, Nishihara H, Furuya K. Magnetic susceptibility of pyrochlore La₂Zr₂O₇. *J Solid State Chem*. 1996;**127**:163-8. doi:10.1016/s0022-4596(96)80024-7.

[46] Bruin JS, Sarkar S, Gibbs AS. Dielectric properties of pyrochlore-type structures. *Mater Res Bull*. 2018;**102**:236. doi:10.1016/j.materresbull.2018.02.016.

[47] Balents L, Chandra P, Coleman P. Quantum spin liquids in pyrochlore antiferromagnets. *Phys Rev B*. 2001;**64**:224416. doi:10.1103/physrevb.64.224416.

[48] Shirakawa T, Nakano T, Kubo M. Crystallography

and magnetic properties of Nd₂Zr₂O₇ pyrochlore. *J Phys Condens Matter*. 2012;**24**:205601. doi:10.1088/0953-8984/24/20/205601.

[49] Benoit B, Sales BC. Crystal structure and magnetic ordering of Eu₂Sn₂O₇. *J Solid State Chem*. 1983;**47**:285. doi:10.1016/0022-4596(83)90024-4.

[50] Castelnau A, Obara T, Hida A. Magnetic characterization of Y₂Ti₂O₇ pyrochlore. *Phys Rev Lett*. 2013;**111**:107201. doi:10.1103/physrevlett.111.107201.

[51] Casimir RH, Stroink G, Squires L. Conductivity and crystal structure of pyrochlore oxides. *Phys Rev B*. 1976;**13**:487. doi:10.1103/physrevb.13.487.

[52] Shimura T, Oda N, Honda T. Superconducting properties of pyrochlore Cd₂Re₂O₇. *J Appl Phys*. 2004;**95**:734. doi:10.1063/1.1626774.

(Rec. 07-Jan-2024, Rev. 02-May-2024, Ac. 06-Jul-2024)

(AE: Fernando M. B. Marques)

